Full Paper

Propellants,
Explosives,
Pyrotechnics

DOI: 10.1002/prep.201700037

Potential Biocides: Iodine-Producing Pyrotechnics

Jimmie C. Oxley,*[a] James L. Smith,[a] Matthew M. Porter,[a] Maxwell J. Yekel,[a] and Jeffrey A. Canaria[a]

Abstract: Currently there is a need for specialized pyrotechnic materials to combat the threat of biological weapons. Materials have been characterized based on their potential to produce heat and molecular iodine gas (I_2) to kill spore-forming bacteria (e.g. anthrax). One formulation, already proven to kill anthrax simulants, is diiodine pentoxide with aluminum; however, it suffers from poor stability and storage problems. The heat and iodine gas output from this mixture and candidate replacement mixtures were measured with bomb calorimetry and extraction and analysis of I_2 by UV-Vis. Of the mixtures analyzed, calcium iodate and aluminum was found to be the highest producer of I_2. The heat output of this mixture and others can be tuned by adding more fuel, with the cost of some iodine. Products of combustion were analyzed by thermal analysis (SDT), XPS, XRD, and LC/MS. Evidence for various metal iodides and metal oxides was collected with these methods.

Keywords: ■Keywords missing!!!■

1 Introduction

Previously we examined a series of oxidizers and fuels to determine their potential as explosive threats [1]. In the current work we examine, in detail, performance of oxides of iodine with the goal of determining their effectiveness as biocides. The biological threat of particular concern is spore production by *Bacillus anthracis*. While kill methods are diverse and not completely understood, it is known that a combination of heat and molecular iodine is effective [2,3]. A number of iodate and periodate salts were examined by formulating them with fuels and measuring heat evolution and molecular iodine release. Diiodine pentoxide has been used as a benchmark because it contains the highest weight percentage of iodine. Unfortunately, its long-term stability with a favored fuel, aluminum, is poor. Herein we examine the fuels aluminum and boron carbide.

2 Experimental Section

2.1 Calorimetry and Iodine (I_2) Quantification

The oxidizers KIO_3, $NaIO_3$, $NaIO_4$, KIO_4 were purchased from Acros; I_2O_5, and $Ca(IO_3)_2$ were purchased from Strem; the aluminum flake (23 μm) and boron carbide (8 μm) fuels were from Obron and Electron Microscopy Sciences, respectively. The oxidizers were sieved to 100–200 mesh (150-75 μm). $Bi(IO_3)_3$ was synthesized according to Zachariah et al and used as prepared [4]. For preparation of $Bi(IO_3)_3$, a solution of $Bi(NO_3)_3{\bullet}5H_2O$ (4.85 g in 80 mL, 2 M nitric acid) was added to HIO_3 solution (5.28 mg in 80 mL H_2O), then rinsed with 600 mL H_2O and 100 mL of methanol. Product was dried under vacuum overnight. Average particle size was 4 μm (Horiba LA950 Particle Size Analyzer, wet mode).

The pyrotechnic mixtures were mixed as dry loose powders using a Resodyne Lab Ram Acoustic Mixer (acceleration 35–40 G). Heat released from the ignition of the pyrotechnic formulations was determined using a Parr 6200 Isoperibol Bomb Calorimeter. The Parr bomb was calibrated (i.e. 10 trials) with benzoic acid ignited with fuse wire (9.6232 J/cm) and cotton string (167.36 J) in 2515 kPa oxygen ($\Delta H_{comb} = 26434$ J/g). In an oxygen atmosphere, the string is in con-tact with the fuse wire and sample, and is ignited by the fuse wire to aid the ignition of the sample. The pyrotechnics (2–3 samples under each set of conditions) were loaded in 2 g samples and ignited with a fuse wire under argon (515 kPa). This slightly elevated pressure was chosen to sim-plify purging of the Parr 1108 bomb with Argon and to en-sure a tight seal. Molecular iodine (I_2) produced from each burn was quantified with ultraviolet-visible (UV-Vis) spectro-scopy (Agilent 8453 spectrometer, 190 to 1100 nm, reso-lution 1 nm, 0.5 s integration time). Iodine was extracted from the bomb with 100 mL of an aqueous 0.5 M potassium iodide (KI) solution. The aqueous solution with excess of I^- was added to solubilize I_2 and transform it to I^{3-} (absorb-ance 353 nm) [5]. Extracts were diluted with known amounts of 0.025 M KI for absorbance measurements at 353 nm to quantify iodine. Control samples were made by pressing solid iodine (0.8 g) with benzoic acid (1.2 g). When these control samples were ignited under 2515 kPa oxygen, iodine recovery was ~ 97 %. For $Bi(IO_3)_3$ mixtures, an interfer-ence in the UV-Vis spectra (Figure S33–S34), attributed to a

---

[a] *J. C. Oxley, J. L. Smith, M. M. Porter, M. J. Yekel, J. A. Canaria*
Department of Chemistry; University of Rhode Island
140 Flagg Road, Kingston, RI, USA 02881
**e-mail: joxley@chm.uri.edu*

Supporting information for this article is available on the WWW under https://doi.org/10.1002/prep.201700037

BiI_3 and KI interaction was observed [6]. For these mixtures, iodine standards and sample extractions were conducted with methylene chloride (at 506 nm), which did not dissolve BiI_3. Control experiments with methylene chloride extractions showed lower recovery (73 %), which was factored into the recovered iodine from $Bi(IO_3)_3$ mixtures.

2.2 Aging Studies

For aging studies, loose powder pyrotechnic mixtures were aged at 60 °C and 75 % RH (relative humidity). Time points were at 3 days and 14 days. Fresh samples and aged samples were analyzed by simultaneous differential scanning calorimetry/thermogravimetric analysis (TA Instruments, Q600 SDT, 20C/min, 50 to 1000 °C); infrared (IR) spectroscopy (Thermo Nicolet 6700 FR-IR with ATR cell, 32 scans, resolution 4 cm^{-1}, 650–4000 cm^{-1}); and visual observation. IR was used specifically to detect oxygen-hydrogen bonds, indicating uptake of water. The burn characteristics of fresh and aged samples were also noted.

2.3 Simultaneous Differential Scanning Calorimetry Thermogravimetric Analysis (SDT)

A TA instruments Q600 SDT was used to characterize the original pyrotechnic mixtures, combustion products (from bomb calorimetry, 515 kPa Argon), and standard mixtures. Samples of 3–5 mg were heated in alumina crucibles at a scan rate of 20 °C/min from 50 to 1000 °C. To remove solid iodine or solvents (in the case of water or methanol extracts for LC/MS) combustion products were dried in a vacuum oven overnight at 50 °C before the analysis. Unless stated otherwise, samples were run under nitrogen.

2.4 Titration for Oxide Content

In the case of 80/20 $Ca(IO_3)_2$/Al combustion products (pH 11 when mixed with water), an acid base titration was performed. Hydrochloric acid (30 mL of 0.100 M) was added to 50–150 mg of combustion products and allowed to stir for 20 min. The solution was then back-titrated with 0.100 M sodium hydroxide, with bromothymol blue indicator.

2.5 X-Ray Photoelectron Spectroscopy (XPS)

A Thermo Scientific K-Alpha XPS (Aluminum source, 1486.7 eV) was used to help determine bomb calorimetry combustion products of $NaIO_3$/Al, $Bi(IO_3)_3$/Al, KIO_3/Al, $Ca(IO_3)_2$/Al, and I_2O_5/Al. The pass energy was 50 eV with a resolution of ±0.05 eV. Samples and standards were prepared in a nitrogen glove box (from Genesis). Charge effects were corrected based on the peak signal from the corresponding cation of an appropriate standard (i.e. KIO_3/Al combustion products were corrected from K2p3/2 from KI).

2.6 Liquid Chromatography/Mass Spectrometry (LCMS)

Water and methanol extracts of bomb calorimetry combustion products of $Ca(IO_3)_2$/Al and I_2O_5/Al were prepared and infused into a Thermo Exactive Orbitrap Mass spectrometer with an electrospray ionization interface (ESI). This method was modified from a method used to analyze aluminum chloride in ESI negative mode with no additives in water [7]. The tune conditions (10 µl/min) were as follows: spray voltage 1.80 kV (for water extracts) and 2.4 kV (for methanol extracts); capillary temperature at 200 °C; sheath gas (N_2) at a flow rate of 8; aux gas (N_2) at a flow rate of 1; capillary voltage at −10 V; tube lens at −175 V, and skimmer voltage at −25 V. The instrument passed the calibration with a mass accuracy of 2 ppm. The mass spec scanned from 128.0 to 600.0 m/z with 25,000 resolution and a maximum injection time of 50 ms. Solid combustion products were extracted with either water (60–75 mg in 10 mL) or methanol (500 mg in 25 mL) in falcon tubes by vortex mixing for 2 min, sonicating for 20 min, vortex mixing again for 2 min, then centrifuging for 10 min at 3.0G.. The methanol extract was decanted from the samples, and diluted with 50/50 v/v methanol/water to a concentration of 500–750 µg/ml. Standard solutions of calcium iodide, aluminum iodide, and calcium oxide were also prepared the same way (50 mg in 10 mL of water or 200 mg in 25 mL of methanol), then diluted to 400 µg/ml with 50/50 methanol/water.

2.7 Powder X-Ray Diffraction

A Rigaku Ultima IV XRD was used (Cu source, 40 kV, 44 mA) to help identify combustion products of the $Ca(IO_3)_2$/Al mixtures. The scan was 0.667 deg/min from 10 to 110 deg at a sampling width of 0.25 deg. Combustion products for 80/20 $Ca(IO_3)_2$/Al and 60/40 $Ca(IO_3)_2$/Al were handled in a glove box, then run in the instrument with containers of drierite in the analysis chamber that had pre-equilibrated for 1 hour.

2.8 Friction Testing (BAM Method)

Testing was conducted according to the UN method (on an FS-12A BAM machine from OZM research) where the threshold initiation level (TIL) of a sample (in N force) is reported where 1 out of 6 samples were a "go" with a snapping sound [8]. A sample size of 10 mm^3 was used.

2.9 Drop-Weight Impact (Modified BOE Method)

This test was conducted with a BOE machine manufactured by SMS (10 mg sample, 3.63 kg weight) using the UN method [8]. $Ca(IO_3)_2/Al$ was tested seven times at the highest height of the instrument (75 cm). A Dh_{50} number was obtained with an up/down method (14 samples, where 50% of the samples were a "go") with RDX (class 1, Holston) for comparison. A test was considered a "go" when an explosion or flash occurred.

2.10 Electrostatic Sensitivity Testing (ARDEC Method 1032)

This test was conducted with a machine manufactured by UTEC Corporation, LLC using ARDEC method 1032 [9]. Testing starting at the 0.25 J level, and the energy level was stepped down until a TIL energy value was reached with 0 out of 20 samples were a "go". A test was considered a "go" when a flash considerably brighter than a blank occurred and the tape holding the sample down split open.

3 Results and Discussion

Choice of oxidizers was governed by availability as well as reported iodine production (Table 1). (Iodoform was considered but not examined because it was neither an oxidizer nor a good fuel.)

Table 1. Iodine Content of Oxidizers Employed

Iodine Sources	mw (g/mol)	# I's	wt % iodine	wt% oxygen
KIO_3	214	1	59	22
$NaIO_3$	198	1	64	24
I_2O_5	334	2	76	24
$Ca(IO_3)_2$	390	2	65	25
$Bi(IO_3)_3$	734	3	52	20
$NaIO_4$	214	1	59	30
KIO_4	230	1	55	28

Because aluminum is often used to create heat-producing pyrotechnic mixtures, oxidizers were initially compared using it as the fuel (Figure 1). Boron carbide was also examined because recent studies reported when it was used in delay mixtures of periodate, iodine production was observed (Figure 2) [10].

As Figure 1 shows, diiodine pentoxide was most effective in both iodine and heat production. However, long term stability was poor. In the presence of moisture this oxide is reportedly converted to iodic acid, also a white solid [11]. The poor stability was exacerbated in the presence of aluminum. After three days, at 60 °C and 75 % relative humidity, the 80/20 I_2O_5/Al mixture turned from a grey powder to a dark brown powder (Figure 3). It may be the reaction of aluminum with iodic acid which causes the rapid color change observable in Figure 3. Evidence of the presence of iodic acid can be found in the SDT of I_2O_5 aged under the same conditions (Figure S2; water loss at 112 °C and 219 °C). At the same temperature and humidity, visual observations as well as infrared spectrometry (IR), thermal gravimetric analysis (TGA), and differential scanning calorimetry (DSC) suggested that calcium iodate, sodium iodate, and sodium periodate, (and mixtures with fuel) were stable (Figure S1-S32). All oxidizers alone remained white solids through the aging study. When an original 75/25 calcium iodate/aluminum mixture was allowed to age two weeks under these conditions, no change is observed in its appearance, production of iodine or thermal trace, suggesting acceptable thermal stability (Figure S22-S24).

Even without considering the efficiency of I_2 production, it would be difficult for other species to match diiodine pentoxide (I_2O_5) in terms of iodine formation because they do not contain as much iodine per mass of oxidizer (Table 1). Several overall reactions are possible (eq. 1–3), where M represents the alkali metal cations in this study.

$$6\ MIO_3 + 10\ Al \rightarrow 5\ Al_2O_3 + 3\,M_2O + 3I_2 \qquad (1)$$

$$MIO_3 + 2\ Al \rightarrow Al_2O_3 + MI \qquad (2)$$

$$6\ MIO_3 + 2\ Al \rightarrow Al_2I_6 + 3\,M_2O + 15/2\ O_2 \qquad (3)$$

The alkali iodates normally decompose to make the iodide salt (eq. 2) and oxygen with perhaps up to 30 % forming the oxide instead (eq. 1) [12]. The addition of a fuel eliminates the free oxygen, but in the case of aluminum fuel, excess aluminum may promote the formation of Al_2I_6 [13]. Six oxidizers and I_2O_5 were examined with aluminum, boron carbide and a mixture of the two (Table 2). The data reported was obtained in an argon atmosphere in a closed-bomb (Parr); iodine (I_2) was collected after combustion and usually quantified by UV-Vis spectroscopy. The reported results are averages of at least three tests. Average heat released under argon (across all mixes) was 3975 J/g; similar to heat released from 80/20 I_2O_5/Al (4414 J/g). Iodine production was more sensitive to the fuel/oxidizer ratio than was heat output (Table 3). Review of the data sorted in Table 3 indicated that as the oxidizer/fuel ratio moved from stoichiometric (roughly 80/20) to a more fuel rich formulation (60/40), I_2 production decreased and heat generally increased. We attributed this to oxygen deficiency, which caused the fuel to combine with the iodine species (acting as oxidant) preventing the release of molecular iodine. Indeed, preliminary data suggested that both iodine production and heat release are improved by the presence of oxygen.

A better understanding of the pyrotechnic reactions, especially knowing why mixes like $Ca(IO_3)_2/Al$ favor iodine production over other mixes, required identification of re-

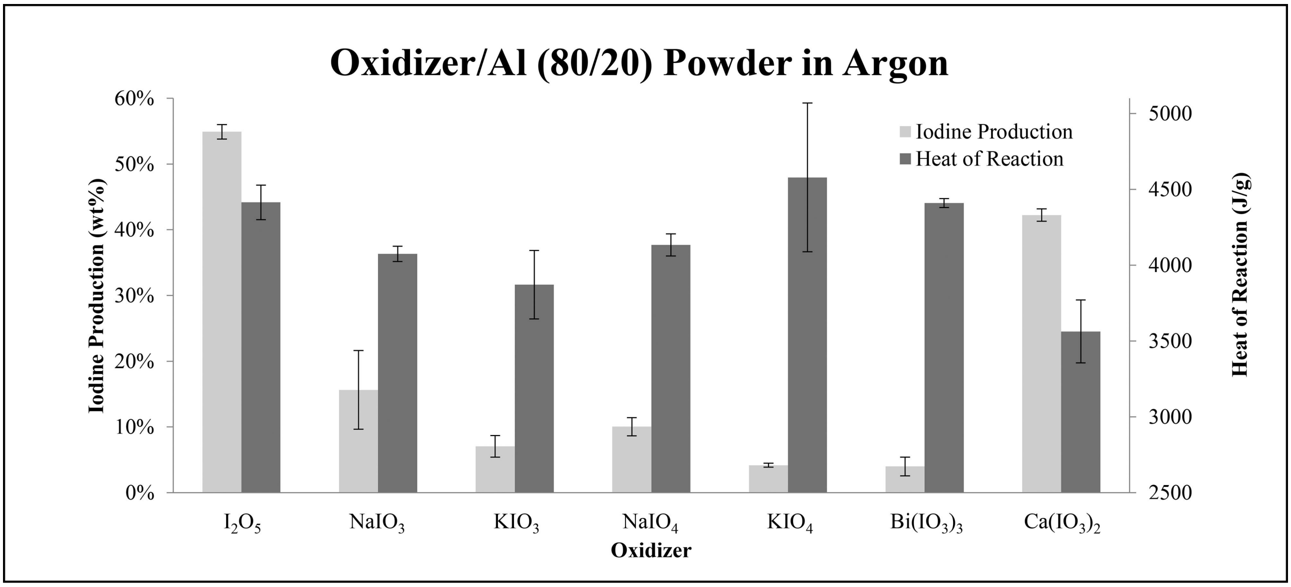

Figure 1. Iodine & heat release from various iodine species burned (closed-bomb) with aluminum.

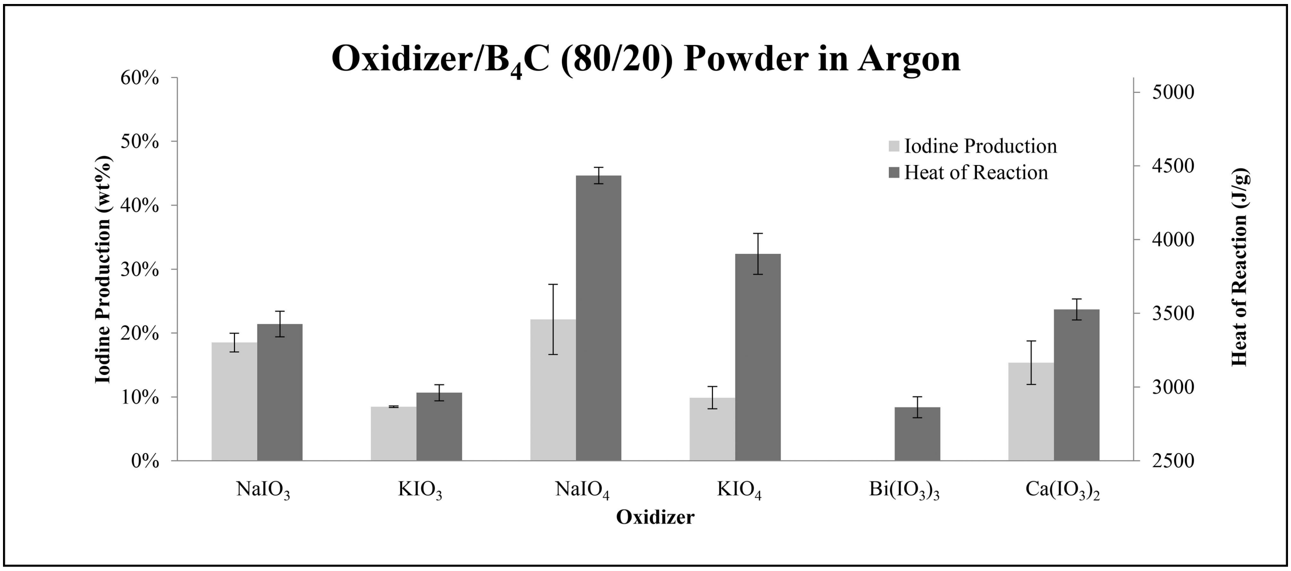

Figure 2. Iodine & heat release from various iodine species burned (closed-bomb) with boron carbide. Diiodinepentoxide did not burn with boron carbide under argon.

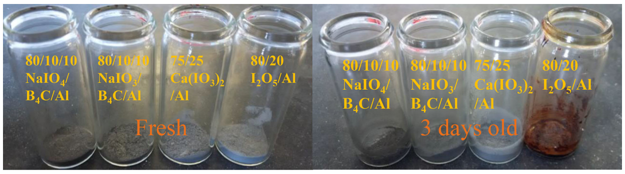

Figure 3. Freshly made (left) and aged 3 days at ambient pyrotechnic mixtures.

action products (by XPS, SDT, XRD, and LC/MS) and ignition mechanisms (by SDT). Measurement of heat evolved and iodine produced was obtained from ignitions in a sealed, Parr bomb calorimeter and extraction of the resulting residue with aqueous KI solution and quantification of iodine by UV-Vis. Other solid products were collected and analyzed by X-ray photoelectron spectroscopy (XPS) and simultaneous thermal gravimetric/differential scanning calorimetry (DSC/SDT). XPS results in Table 4 show electron binding energies of the combustion products, which are consistent with oxidation state assignments of I^-, O^{2-}, Al^{+3}, Ca^{+2}, N^{3-}, Na^+, K^+,

Table 2. Iodate salts with Various Fuels 2 g in Bomb Calorimeter (515 kPa Argon)-Heat & I_2 Evolved

Mix Info	Oxidizer	Oxidizer (mass frac)	Al (23um) (mass frac)	Fuel 2	Fuel 2 (mass frac)	Theoretical Iodine tot (wt%)	I_2 Recovered (wt%)	Std Dev	I_2 Yield /Theory	Std Dev	Heat Rxn (J/g)	Std Dev
60/40 $Bi(IO_3)_3/Al$	$Bi(IO_3)_3$	0,60	0,40	–	–	31%	1%	–	2%	–	4129	56
80/20 $Bi(IO_3)_3/Al$	$Bi(IO_3)_3$	0,80	0,20	–	–	42%	4%	1%	7%	2,5%	4410	30
80/20 $Bi(IO_3)_3/Al$ (2515 kPa)	Bi(IO3)3	0,80	0,20	–	–	42%	0%	0%	1%	1,2%	4367	9
80/20 $Bi(IO_3)_3/B_4C$	$Bi(IO_3)_3$	0,80	–	B_4C	0,20	42%	0%	–	0%	–	2863	71
80/10/10 $Bi(IO_3)_3/Al/B_4C$	$Bi(IO_3)_3$	0,80	0,10	B_4C	0,10	42%	0%	0%	1%	0,8%	3552	76
60/40 $Ca(IO_3)_2/Al$	$Ca(IO_3)_2$	0,60	0,40	–	–	39%	2%	1%	5%	2,2%	4444	147
70/30 $Ca(IO_3)_2/Al$	$Ca(IO_3)_2$	0,70	0,30	–	–	46%	15%	5,9%	34%	12,8%	4667	44
75/25 $Ca(IO_3)_2/Al$	$Ca(IO_3)_2$	0,75	0,25	–	–	49%	36%	3%	73%	7,0%	4491	136
80/20 $Ca(IO_3)_2/Al$	$Ca(IO_3)_2$	0,80	0,20	–	–	52%	42%	1%	81%	1,8%	3563	208
80/20 $Ca(IO_3)_2/Al$ (2515 kPa)	Ca(IO3)2	0,80	0,20	–	–	52%	45%	2%	86%	3,0%	3551	292
70/10/20 $Ca(IO_3)_2/B_4C/Al$	$Ca(IO_3)_2$	0,70	0,20	B_4C	0,10	46%	23%	–	50%	–	4073	–
80/20 $Ca(IO_3)_2/B_4C$	$Ca(IO_3)_2$	0,80	–	B_4C	0,20	52%	15%	3%	29%	6,6%	3526	71
80/10/10 $Ca(IO_3)_2/Al/B_4C$	$Ca(IO_3)_2$	0,80	0,10	B_4C	0,10	52%	40%	2%	78%	4,7%	3867	58
80/20 $Ca(IO_3)_2/Al$ + 10% C	$Ca(IO_3)_2$	0,72	0,18	C	0,10	47%	6%	2%	14%	3,3%	3237	9
80/20 $Ca(IO_3)_2/Al$ + 5% C	$Ca(IO_3)_2$	0,76	0,19	C	0,05	49%	23%	5%	46%	10,4%	3535	38
60/40 KIO_3/Al	KIO_3	0,60	0,40	–	–	39%	0%	–	0%	–	4461	50
80/20 KIO_3/Al	KIO_3	0,80	0,20	–	–	47%	7%	2%	15%	3,4%	3871	226
80/20 KIO_3/B_4C	KIO_3	0,80	–	B_4C	0,20	47%	8%	0%	18%	0,3%	2962	55
80/10/10 $KIO_3/Al/B_4C$	KIO_3	0,80	0,10	B_4C	0,10	47%	14%	0%	30%	0,8%	3754	84
70/20/10 $KIO_4/B_4C/Al$	KIO_4	0,70	0,10	B_4C	0,20	39%	8%	–	20%	–	4608	–
80/20 KIO_4/Al	KIO_4	0,80	0,20	–	–	44%	4%	0%	9%	0,7%	4578	490
80/20 KIO_4/B_4C	KIO_4	0,80	–	B_4C	0,20	44%	10%	2%	22%	3,9%	3903	139
80/10/10 $KIO_4/Al/B_4C$	KIO_4	0,80	0,10	B_4C	0,10	44%	20%	2%	46%	3,5%	4946	71
60/40 $NaIO_3/Al$	$NaIO_3$	0,60	0,40	–	–	39%	0%	–	0%	–	4881	151
75/25 $NaIO_3/Al$	$NaIO_3$	0,75	0,25	–	–	48%	6%	–	12%	–	5182	–
80/20 $NaIO_3/Al$	$NaIO_3$	0,80	0,20	–	–	51%	16%	6%	30%	11,7%	4074	51
80/20 $NaIO_3/Al$ (2515 kPa)	NaIO3	0,80	0,20	–	–	51%	28%	1%	54%	1,1%	4058	21
85/15 $NaIO_3/Al$	$NaIO_3$	0,85	0,15	–	–	55%	15%	–	28%	–	2911	–
75/5/20 $NaIO_3/Al/B_4C$	$NaIO_3$	0,75	0,05	B_4C	0,20	48%	11%	1%	23%	2,9%	3765	13
80/5/15 $NaIO_3/Al/B_4C$	$NaIO_3$	0,80	0,05	B_4C	0,15	51%	26%	1%	51%	1,3%	3592	26
85/5/10 $NaIO_3/Al/B_4C$	$NaIO_3$	0,85	0,05	B_4C	0,10	55%	28%	1%	51%	0,9%	3219	24
75/10/15 $NaIO_3/Al/B_4C$	$NaIO_3$	0,75	0,10	B_4C	0,15	48%	17%	–	35%	–	4014	–
80/10/10 $NaIO_3/Al/B_4C$	$NaIO_3$	0,80	0,10	B_4C	0,10	51%	22%	3%	43%	5,1%	3997	34
85/10/5 $NaIO_3/Al/B_4C$	$NaIO_3$	0,85	0,10	B_4C	0,05	55%	30%	–	55%	–	3511	–
80/20 $NaIO_3/B_4C$	$NaIO_3$	0,80	–	B_4C	0,20	51%	19%	1%	36%	2,8%	3427	87
65/35 $NaIO_4/B_4C$	$NaIO_4$	0,65	–	B_4C	0,35	39%	3%	2%	7%	4,0%	4044	95
70/30 $NaIO_4/B_4C$	$NaIO_4$	0,70	–	B_4C	0,30	42%	4%	0%	10%	1,1%	4204	72
75/25 $NaIO_4/B_4C$	$NaIO_4$	0,75	–	B_4C	0,25	44%	9%	2%	20%	3,4%	4468	30
70/20/10 $NaIO_4/B_4C/Al$	$NaIO_4$	0,70	0,10	B_4C	0,20	42%	11%	–	28%	–	4932	–
80/20 $NaIO_4/Al$	$NaIO_4$	0,80	0,20	–	–	47%	10%	1%	21%	2,9%	4134	73

Table 2. continued

Mix Info	Oxidizer	Oxidizer (mass frac)	Al (23um) (mass frac)	Fuel 2	Fuel 2 (mass frac)	Theoretical Iodine tot (wt%)	I_2 Recovered (wt%)	Std Dev	I_2 Yield /Theory	Std Dev	Heat Rxn (J/g)	Std Dev
80/10/10 $NaIO_4$/B_4C/Al	$NaIO_4$	0,80	0,10	B_4C	0,10	47%	31%	–	66%	–	5038	–
80/20 $NaIO_4$/B_4C	$NaIO_4$	0,80	–	B_4C	0,20	47%	22%	5%	47%	11,5%	4434	55
80/20 I_2O_5/Al	I_2O_5	0,80	0,20	–	–	61%	55%	1%	90%	1,8%	4414	114
60/40 I_2O_5/Al	I_2O_5	0,60	0,40	–	–	46%	0%	–	0%	–	5789	173
80/20 I_2/Al	I_2	0,80	0,20	–	–	80%	0%	–	0%	–	882	–

Theoretical iodine (wt%) is iodine content of original mixture; I_2 recovered (wt%) is mass I_2 extracted from combustion products (quantification by UV-Vis) relative to original mix mass; I_2 yield /theory is mass of I_2 relative to theoretical amount.

Table 3. Select Parr Calorimetry Results: Effect of Oxidizer/ Fuel Ratio on Iodine and Heat Production.

Mix Info	Oxidizer	Oxidizer (mass frac)	Al (23um) (mass frac)	Fuel 2	Fuel 2 (mass frac)	Theoretical Iodine tot (wt%)	% I_2 g /g mix	Std Dev	I_2 Yield/ Theory	Std Dev	Heat Rxn (J/g)	Std Dev
85/15 $NaIO_3$/Al	$NaIO_3$	0,85	0,15	–	–	55%	15%	–	28%	–	2911	–
80/20 $NaIO_3$/Al	$NaIO_3$	0,80	0,20	–	–	51%	16%	6,0%	30%	11,7%	4074	51
75/25 $NaIO_3$/Al	$NaIO_3$	0,75	0,25	–	–	48%	6%	–	12%	–	5182	–
60/40 $NaIO_3$/Al	$NaIO_3$	0,60	0,40	–	–	39%	0%	–	0%	–	4881	151
80/20 $NaIO_4$/B_4C	$NaIO_4$	0,80	–	B_4C	0,20	47%	22%	5,5%	47%	11,5%	4434	55
75/25 $NaIO_4$/B_4C	$NaIO_4$	0,75	–	B_4C	0,25	44%	9%	1,5%	20%	3,4%	4468	30
70/30 $NaIO_4$/B_4C	$NaIO_4$	0,70	–	B_4C	0,30	42%	4%	0,4%	10%	1,1%	4204	72
65/35 $NaIO_4$/B_4C	$NaIO_4$	0,65	–	B_4C	0,35	39%	3%	1,6%	7%	4,0%	4044	95
80/20 $Ca(IO_3)_2$/Al	$Ca(IO_3)_2$	0,80	0,20	–	–	52%	42%	0,9%	81%	1,8%	3563	208
75/25 $Ca(IO_3)_2$/Al	$Ca(IO_3)_2$	0,75	0,25	–	–	49%	36%	3,4%	73%	7,0%	4491	136
70/30 $Ca(IO_3)_2$/Al	$Ca(IO_3)_2$	0,70	0,30	–	–	46%	15%	5,9%	34%	12,8%	4667	44
60/40 $Ca(IO_3)_2$/Al	$Ca(IO_3)_2$	0,60	0,40	–	–	39%	2%	0,9%	5%	2,2%	4444	147
85/10/5 $NaIO_3$/Al/B_4C	$NaIO_3$	0,85	0,10	B_4C	0,05	55%	30%	–	55%	–	3511	–
85/5/10 $NaIO_3$/Al/B_4C	$NaIO_3$	0,85	0,05	B_4C	0,10	55%	28%	0,5%	51%	0,9%	3219	24
80/10/10 $NaIO_3$/Al/B_4C	$NaIO_3$	0,80	0,10	B_4C	0,10	51%	22%	2,6%	43%	5,1%	3997	34
80/5/15 $NaIO_3$/Al/B_4C	$NaIO_3$	0,80	0,05	B_4C	0,15	51%	26%	0,7%	51%	1,3%	3592	26
75/10/15 $NaIO_3$/Al/B_4C	$NaIO_3$	0,75	0,10	B_4C	0,15	48%	17%	–	35%	–	4014	–
75/5/20 $NaIO_3$/Al/B_4C	$NaIO_3$	0,75	0,05	B_4C	0,20	48%	11%	1,4%	23%	2,9%	3765	13

Bi^{+3}. The resulting elemental analysis is shown in Table 5, noting that all results show more oxygen than anticipated. This is attributed to the presence of moisture or surface oxidation; oxidation of iodides is explained later from SDT experiments (Table 7). The roughly 1:1 match of Na and K to I (from mixes 55, 53, and NaI) and the roughly 1:3 match for Bi to I (from mix 97) suggest that these cations become incorporated in iodide salts. However, for $Ca(IO_3)_2$/Al from mix 60 (which is stoichiometric) there is not sufficient iodide (I^-) found to support the required 1:2 ratio for CaI_2. When the

Table 4. XPS on Combustion Products- 2 g Iodates with Al in Bomb Calorimeter (Argon).

Combustion				Qualitative Analysis of Peak Binding Energy (eV)													Correction
Product	Oxidizer	%	% Al	I3d5/2	I3d3/2	O1s	Al2p	Al2p	N1s	Ca2p3/2	Ca2p1/2	Na1s	K2p3/2	Bi4f5/2 (higher number)	Bi4f7/2	Correction	Type
Mix 60	$Ca(IO_3)_2$	80	20	618,6	630,0	531,0	74,0			347,2	350,9					−0,91	Ca2p3/2 CaO
Mix 78	$Ca(IO_3)_2$	60	40	618,7	630,2	531,5	74,2			347,2	350,9					−0,91	Ca2p3/2 CaO
Mix 54	I_2O_5	80	20	619,9	631,4	532,4	75,4									0,57	Al2p AlI3
Mix 95	I_2O_5	60	40	619,1	630,6	532,8	75,4									0,36	Al2p AlI3
Mix 97	$Bi(IO_3)_3$	80	20	619,4	630,9	531,8	75,1							164,6	159,3	0,22	Bi4f5/2 BiI3
Mix 116	$Bi(IO_3)_3$	60	40	619,4	630,9	533,0	75,6							164,6	159,3	−0,01	Bi4f5/2 BiI3
Mix 55	KIO_3	80	20	619,3	630,8	530,1	73,2						293,1			−0,17	K2p3/2 KI
Mix 115	KIO_3	60	40	619,3	630,8	530,8	73,9						293,1			−0,94	K2p3/2 KI
Mix 53	$NaIO_3$	80	20	619,2	630,7	531,2	73,9					1071,9				−1,12	Na1 s NaI
Mix 114	$NaIO_3$	60	40	618,8	630,3	530,7	73,6					1071,9				−1,48	Na1 s NaI
Standards																	
Al						531,3	74,0	71,3								−0,33	O1 s Al2O3
Al heated in Air						531,3	74,2									−0,07	O1 s Al2O3
Al heated in N_2						531,3	73,7		396,7							−0,23	O1 s Al2O3
Al_2O_3						531,3	75,0										
CaO						531,5				347,2	350,8						
CaI_2				618,8	630,2	531,4				347,2	350,8					−1,83	Ca2p3/2 CaO
AlI_3				619,3	630,7	532,8	75,4										
KI				619,4	630,9	531,3							293,1				
NaI				619,1	630,6	534,9						1071,9					
BiI_3				619,6	631,1	531,7								164,6	159,3		
$Ca(IO_3)_2$				624,3	635,8	531,3				347,2	351,0					−0,46	Ca2p3/2 CaO
$NaIO_3$				624,9	636,4	531,4						1071,9				0,19	Na1 s NaI
$NaIO_4$				625,4	636,8	531,7						1071,9				0,47	Na1 s NaI
KIO_3				624,2	635,7	530,8							293,1			0,97	K2p3/2 KI
$Bi(IO_3)_3$				624,0	635,5	530,5								164,6	159,3	−0,21	Bi4f5/2 BiI3
I_2O_5				624,5	635,98	531,07											
Oxidation State				I^-		O^{-2}	Al^{+3}		N^{-3}	Ca^{+2}		Na^+	K^+	Bi^{+3}			

Table 5. XPS Elemental Analysis-Combustion Products of Iodates with Al.

Combustion Product	Oxidizer	%	%Al	Elemental Analysis (Atomic %) I	O	Al	N	Ca	Na	K	Bi	Sum
Mix 60	$Ca(IO_3)_2$	80	20	4	60	32		3				100
Mix 78	$Ca(IO_3)_2$	60	40	15	53	26		7				100
Mix 54	I_2O_5	80	20	2	59	40						100
Mix 95	I_2O_5	60	40	8	60	32						100
Mix 97	$Bi(IO_3)_3$	80	20	8	56	34					2	100
Mix 116	$Bi(IO_3)_3$	60	40	17	58	24					2	100
Mix 55	$K(IO_3)$	80	20	17	40	25				19	.	100
Mix 115	$K(IO_3)$	60	40	16	42	26				16		100
Mix 53	$Na(IO_3)$	80	20	17	41	22			20			100
Mix 114	$Na(IO_3)$	60	40	10	51	31			8			100
Standards												
$Bi(IO_3)_3$				22	68						10	100
Al					62	38	0					100
Al heated in Air					62	38	0					100
Al heated in N_2					36	43	21					100
Al_2O_3					63	37						100
CaO					74			26				100
CaI_2				54	26			21				100
AlI_3				15	58	27						100
NaI				53					47			100

aluminum fuel content was raised from 20 wt% to 40 wt%, the ratio was consistent with CaI_2 production, but this evidence was not supported by DSC/SDT of the fresh combustion products. However, SDT of dried methanol extracts of the combustion products of 60/40 $Ca(IO_3)_2$/Al did show both decomposition before endothermic mass loss before 200 °C and a melt at 774 °C, characteristic of the presence of both Al_2I_6 and CaI_2 respectively. A dried methanol solution of 50/50 CaI_2/Al_2I_6 was very similar (Figure 4); furthermore, it was demonstrated by LC/MS that CaO (a combustion product) in the presence of Al_2I_6 and moisture can be converted to CaI_2 *vide infra.*

The SDT allowed observation of heat released or absorbed concomitant with weight loss in the iodine-containing samples during heating as opposed to burning with fuel. Table 6 summarizes the observations when these fresh samples were heated in unsealed SDT pans. Table 7 analyzes the remaining solid products produced from the reactions outlined in Table 6 although the actual residue was collected from the bomb calorimetry experiments (Table 2). Under SDT heating, I_2O_5 decomposed at ~438 °C and did not appear to react with aluminum (Figure S4). With or without fuel, both sodium and potassium periodate exothermically reduced to the iodate; for $NaIO_4$ at ~312 °C and for KIO_4 at ~350 °C. After that the thermal scans of both salts were identical to those of their respective iodates [12]. Sodium iodate melts at ~422 °C and decomposes to oxygen and the iodide salt NaI ~600 °C; while potassium iodate undergoes a melt with decomposition to KI at ~550 °C. These changes are endothermic. If aluminum alone is the fuel, the formation of NaI occurs 50° earlier at 550 °C, but that of KI remains at 550 °C and both decompositions remain endothermic. When boron carbide was present alone or with aluminum, the reaction at 550 °C for both $NaIO_3$ and KIO_3 became extremely exothermic (1700 to 2400 J/g) with sodium salt being more energetic than potassium salt. Evidence for KI formation in these boron carbide mixtures was seen by the presence of its melt at 673 °C and evaporation at 750 °C. Comparable evidence of NaI in the boron carbide mixtures was not observed. Boron carbide reacted with the alkali iodates at temperatures (i.e. ~550 °C) much lower than it reacted with air (~770 °C). However, if aluminum alone was the fuel, then NaI and KI melts were observed; the latter, KI at ~676 °C, separated from the Al melt. NaI and Al both exhibit endotherms near 650 °C. This endotherm was interpreted as the melt of NaI if continued heating resulted in significant weight loss. When Al was heated with no added salt it exhibited a neat melting endotherm at 650 °C, but also an exotherm near 850 °C, which we interpret as the formation of AlN. This exotherm was also observed when Al

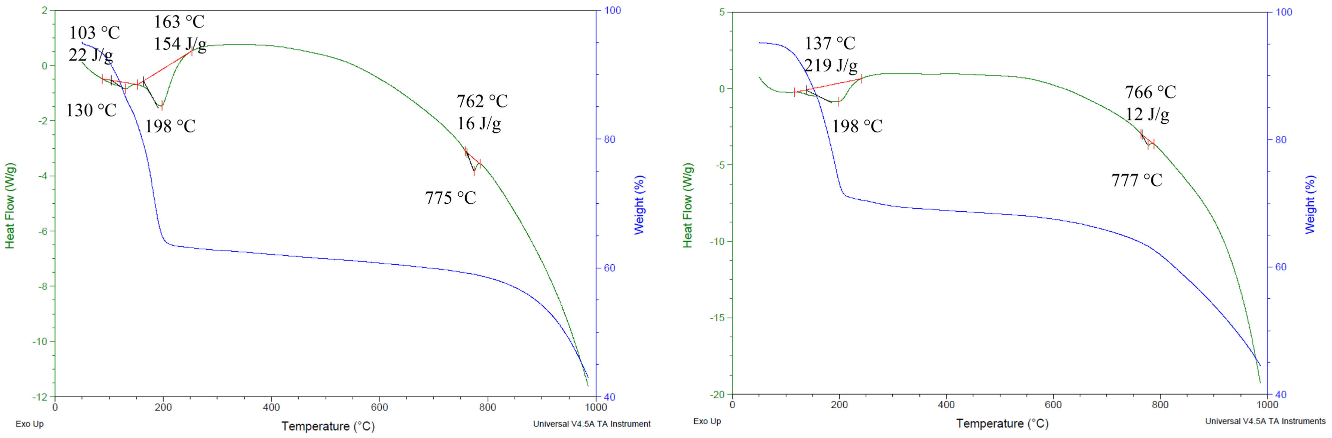

Figure 4. SDT of Dried Methanol Extract of 60/40 $Ca(IO_3)_2$ /Al combustion products (left) and 50/50 CaI_2/Al_2I_6(right).

Table 6. SDT Scans of Various Iodates and Fuels (20 °C/min, 3–5 mg under N_2 unless otherwise stated).

wt% / material	°C	J/g	wt % loss	°C	J/g	wt % loss	°C	J/g	wt % loss	°C	J/g	wt % loss	°C	J/g	wt % loss	°C	J/g	wt % loss	°C	J/g	wt % loss
100 **$NaIO_3$**				425 melt $NaIO_3$	158	0				601 -> NaI + O_2	486	-41	654 melt NaI	11	0	883 NaI Evap	172	-55			
80/20 $NaIO_3$/Al				422 melt $NaIO_3$	113	0	555 -> NaI + O_2	412	-28				657 melt NaI,Al	105	0	722 NaI Evap	27	-48	~850 AlN	-710	3
80/10/10 $NaIO_3$/Al/B_4C				422 melt $NaIO_3$	81	0	547 ->NaBOs+?	-2375	-52				653 melt Al	16	0						
80/20 $NaIO_3$/B_4C				423 melt $NaIO_3$	121	0	547 -> NaBOs+?	-2243	-60				no further peaks								
100 **$NaIO_4$**	312 -> $NaIO_3$ + O_2	-194	-26	425 melt $NaIO_3$	107	0				604 -> NaI + O_2	418	-25	656 melt NaI	26	0	800 NaI Evap		-37			
80/20 $NaIO_4$/Al	312 -> $NaIO_3$ + O_2	-167	-13	423 melt $NaIO_3$	60	0	548 -> NaI + O_2	208	-19				657 melt NaI,Al	78	0	850 NaI Evap		-39	~860 AlN	-29	1
80/10/10 $NaIO_4$/Al/B_4C	310 -> $NaIO_3$ + O_2	-135	-13	422 melt $NaIO_3$	54	0	518 ->NaBOs+?	-1643	-35				653 melt Al	21	0						
80/20 $NaIO_4$/B_4C	312 -> $NaIO_3$ + O_2	-156	-15	425 melt $NaIO_3$	76	0	543 -> NaBOs+?	-1727	-43				no further peaks								
100 **KIO_3**							553 melt KIO_3-> KI + O_2	747	-25				676 melt KI	76	0	847 evap KI	323	-68			
80/20 KIO_3/Al							551 melt KIO_3-> KI + O_2	363	-15	654 Al melt	47	0	676 melt KI	40	0	850 evap KI		-48	~860 AlN	-59	3
80/10/10 KIO_3/Al/B_4C							570 ->KBOs+?	-862	-25	653 Al melt	11	0	672 melt KI	38	0	850 evap KI		-46	~900 AlN	-87	0
80/20 KIO_3/B_4C							566 ->KBOs+?	-1106	-26				673 melt KI	23	0	750 evap KI		-40			
100 **KIO_4**	354 -> KIO_3 + O_2	-95	-40				548 melt KIO_3-> KI + O_2	371	-13				675 melt KI	44	0	813 evap KI	31	-40			
80/20 KIO_4/Al	354 -> KIO_3 + O_2	-124	-25				552 melt KIO_3-> KI + O_2	311	-12	655 Al melt	30	0	677 melt KI	35	0	862 evap KI	195	-40			
80/10/10 KIO_4/Al/B_4C	343 -> KIO3 + O2	-90	-21				562 ->KBOs+?	-770	-19	653 Al melt	8	0	673 melt KI	23	0	850 evap KI		-31	~900 AlN	-37	0
80/20	352	-84	-34				567	-738	-19				674	18	0						

Table 6. continued

wt% / material	°C	J/g	wt % loss	°C	J/g	wt % loss	°C	J/g	wt % loss	°C	J/g	wt % loss	°C	J/g	wt % loss	°C	J/g	wt % loss	°C	J/g	wt % loss
KIO_4/B_4C	-> KIO3 + O2						-> KBOs + ?						melt KI								
100 **$Bi(IO_3)_3$**							550 -> $Bi_5O_7I + I_2 + O_2$	83	-38	579 -> $Bi_2O_3 + I_2$	132	-20				818 melt Bi_2O_3	6	-5			
80/20 $Bi(IO_3)_3/Al$							528 -> $Bi_5O_7I + I_2 + O_2$	24	-27	566 -> $Bi_2O_3 + I_2$	100,8	-16	641 Al -> Al_2O_3 + BiI_3	-196	0						
80/10/10 $Bi(IO_3)_3/Al/B_4C$							547 -> $Bi_5O_7I + I_2 + O_2$	49	-28	583 -> $Bi_2O_3 + I_2$	31	-17	620 Al -> Al_2O_3 + BiI_3	-90	0						
80/20 $Bi(IO_3)_3/B_4C$							547 -> $Bi_5O_7I + I_2 + O_2$?	18	-29	582 -> BiBOs?	-392	-19									
100 **$Ca(IO_3)_2$**													656 -> $Ca_5(IO_6)_2 + I_2 + O_2$	586	-64	736 -> $CaO + I_2 + O_2$	329	-19			
75/25 $Ca(IO_3)_2/Al$													646 -> $CaO + Al_2O_3 + I_2$	-842	-73						
80/10/10 $Ca(IO_3)_2/Al/B_4C$													657 -> CaO + Al2O3 + I2	-572	-80						
80/20 $Ca(IO_3)_2/B_4C$													682 -> $Ca_5(IO_6)_2 + I_2 + O_2$	155	-51	752 -> CaBOs?	-35	-14			
100 **I_2O_5**	200 water loss		-0,5	438 -> $I_2 + O_2$	640	-99															
80/20 I_2O_5/Al	200 water loss		-0,7	428 -> $I_2 + O_2$	148	-76				655 Al melt	21	0									
Al in N_2										657	190	0	Al melt				$2Al + N_2$ -> 2AlN		843	-5989	32
Al in air										635	-3902	19	$Al + O_2$ -> Al_2O_3								
Al/I_2 (50/50)	99	-46	-46	$Al + I_2$ -> Al_2I_6						656	98	0	Al melt								
B_4C in N_2																no thermal event					
B_4C in air																774	-10297	59			
B_4C/I_2 (50/50)	109	47	-53	I_2 evap																	
Bi_2O_3/Al (80/20)										651	28	0	Al melt			732	12	0	813	-281	-18

Table 7. SDT Solid Bomb Combustion Products (20 °C/min, 3–5 mg in N_2 unless otherwise stated).

wt%	material	°C	J/g	wt % loss	°C	J/g	wt % loss	°C Al melt	J/g	wt % loss	°C iodide melt	J/g	wt % total mass loss	XPS	pH
80/20	$Ca(IO_3)_2$/Al										a		−6	Ca^{2+}, Al^{3+}, I^-, O^{2-}	11
60/40	$Ca(IO_3)_2$/Al				300		−10	652	48	0	a		−31	Ca^{2+}, Al^{3+}, I^-, O^{2-}	5
100	CaI_2 in N_2	179	142	−7	$-H_2O$						783	123	−38		
100	CaI_2 in Air	177	104	−8	520	−40	−70								
80/20	$NaIO_3$/Al										649	38	−38	Na^+, Al^{3+}, I^-, O^{2-}	13
60/40	$NaIO_3$/Al										656	28	−46	Na^+, Al^{3+}, I^-, O^{2-}	6
100	NaI in N_2										657	171	−100		
100	NaI in Air										659	104	−93		
80/20	KIO_3/Al										681	31	−53	K^+, Al^{3+}, I^-, O^{2-}	6
60/40	KIO_3/Al							652	14	0	680	28	−42	K^+, Al^{3+}, I^-, O^{2-}	6
100	KI in N_2										681	64	−98		
100	KI in Air										682	108	−96		
80/20	$Bi(IO_3)_3$/Al				365	39	−44				b		−44	Bi^{3+}, Al^{3+}, I^-, O^{2-}	4
60/40	$Bi(IO_3)_3$/Al				320	8	−23	648	10	0	b		−40	Bi^{3+}, Al^{3+}, I^-, O^{2-}	4
100	BiI_3 in N_2		melt evap BiI_3		390	199	−100								
100	BiI_3 in Air		melt evap BiI_3		379	136,1	−97								
80/20	I_2O_5/Al												−4	Al^{3+}, I^-, O^{2-}	6
60/40	I_2O_5/Al				300		−21	648	16	0	c		−24	Al^{3+}, I^-, O^{2-}	4
100	Al_2I_6 in N_2	190	19	−18	258	16	−58	649	5	0					
100	Al_2I_6 in Air	150	84	−43	238	−524	−29								

a. CaI_2 melt at 783 °C was not observed; b. DSC melt & UV-Vis suggests BiI_3; c. Al_2I_6 observed when aluminum in excess.

was the only fuel combined with sodium or potassium iodates/periodates. If aluminum was heated in air, the exotherm is observed much earlier just above 600 °C, and was interpreted as the formation of Al_2O_3. For the iodates equation 2 can be broken into several steps where M is either sodium or potassium cation:

$$MIO_3 + 2\ Al \rightarrow MI + 2\ Al + 3/2\ O_2 \rightarrow Al_2O_3 + MI \quad (4)$$

While NaI and KI have been identified from the DSC melt and XPS examination of the combustion products, we know also from the basicity of the combustion products and presence of molecular iodine that equation 1 is also operative [12,14]. The sodium and potassium salts show an increase in iodine production when boron carbide, rather than aluminum, was used as the fuel (Figures 1 and 2, Tables 2 and 3).

Bismuth triiodate, upon heating, exhibited two modest endotherms at 550 °C and at 579 °C [4,15]. These are assigned as the stepwise oxidation of bismuth iodate to the oxide Bi_2O_3 with release of I_2 (eq. 5, 6). Indeed there was also one small endotherm at 817 °C, the melting point of Bi_2O_3 [16].

$$5Bi\ (IO_3)_3 \rightarrow Bi_5O_7I + 7I_2 + 19O_2 \quad (5)$$

$$2Bi_5O_7I + 1/2O_2 \rightarrow 5Bi_2O_3 + I_2 \quad (6)$$

When aluminum was added the two endotherms were visible at slightly lower temperatures, 528 °C and 566 °C (ac-

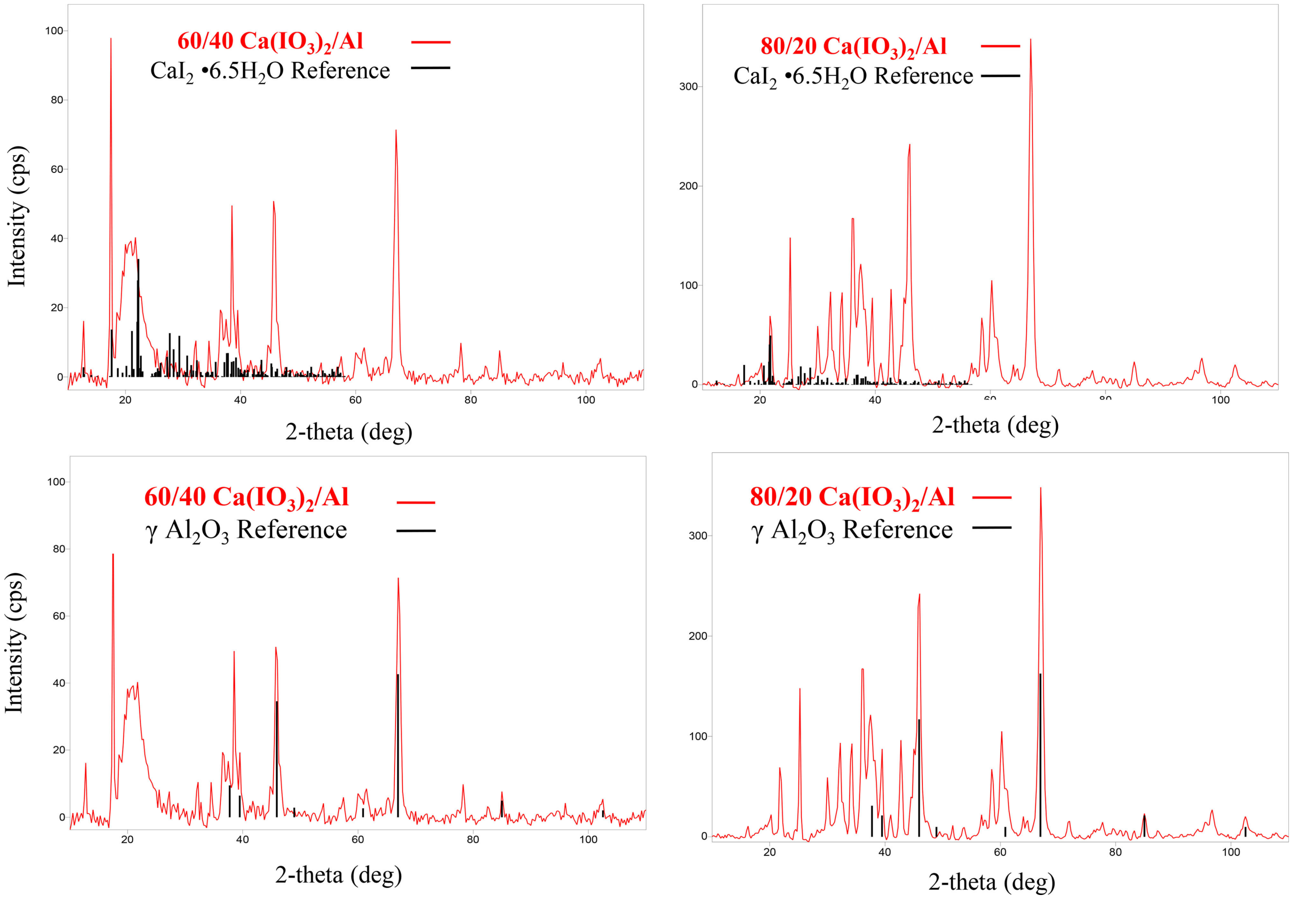

Figure 5. XRD of combustion products of 80/20 $Ca(IO_3)_2$ /Al (left) and 60/40 $Ca(IO_3)_2$ /Al (right).

companied by ~40% weight loss), and an exotherm near the melting point of aluminum (641 °C) appeared. There is little heat released at this exotherm and almost no weight loss (Table 6). This cannot be explained by a direct reaction of Bi_2O_3 with Al. When reagent grade Bi_2O_3 and Al were examined under the same experimental conditions, no reaction was observed until the oxide melted (814 °C). The combustion of bismuth triiodate with aluminum in a sealed vessel under argon yielded a black product that exhibited only one endotherm at ~365 °C. This melt as well as its UV-Vis spectrum confirmed this product as BiI_3 (m.p. 390 °C) [6,16]. Indeed, little molecular iodine was produced if the combustion was in an inert atmosphere. Unlike the alkali iodate salts, less, rather than more, molecular iodine was produced when the bismuth or calcium iodates were burned with boron carbide rather than aluminum (Table 2).

Calcium iodate, like the bismuth iodate, exhibited two modest endotherms at 656 °C and 736 °C. The first endotherm is ascribed to the decomposition of $Ca(IO_3)_2$ to $Ca_5(IO_6)_2$, iodine and oxygen and the second endotherm to the complete oxidation of the calcium salt to calcium oxide with further generation of iodine and oxygen [12,17]. When aluminum is mixed with the calcium iodate, where the decomposition of $Ca(IO_3)_2$ and melt of aluminum coincide at 650 °C, an exothermic reaction occurs which forms both calcium and aluminum oxide as well as iodine (Table 6). The formation of calcium oxide is claimed based on the basicity of the combustion product (from closed bomb calorimetry in argon) from the 80/20 $Ca(IO_3)_2$/Al mixture (pH 11), the ratio of elements in the XPS (Table 5, mix 60); and the fact that when the residue from the combustion was examined by SDT, neither endotherms nor exotherms were observed and weight loss was only 6%. These combustion products were shown by titration to form 11% CaO (assuming this is the product). Some XRD peaks characteristic of γ-Al_2O_3 were observed in the 80/20 $Ca(IO_3)_2$/Al combustion products, but no good matches for a particular iodide (although some peaks match for $CaI_2{\cdot}6.5H_2O$). If aluminum was introduced into the calcium iodate in excess, e.g. 60/40 $Ca(IO_3)_2$/Al, then the DSC/SDT scan of the product mixture showed an endotherm at 652 °C, characteristic of the melt of excess aluminum. XRD peaks of these products match γ-Al_2O_3 and more closely with $CaI_2{\cdot}6.5H_2O$ than the products of the 80/20 $Ca(IO_3)_2$/Al mix (Figure 5). Furthermore, the SDT of the combustion products shows a mass loss of 31%, rather than 6%, and the pH was pH 5, instead of 11. These observations

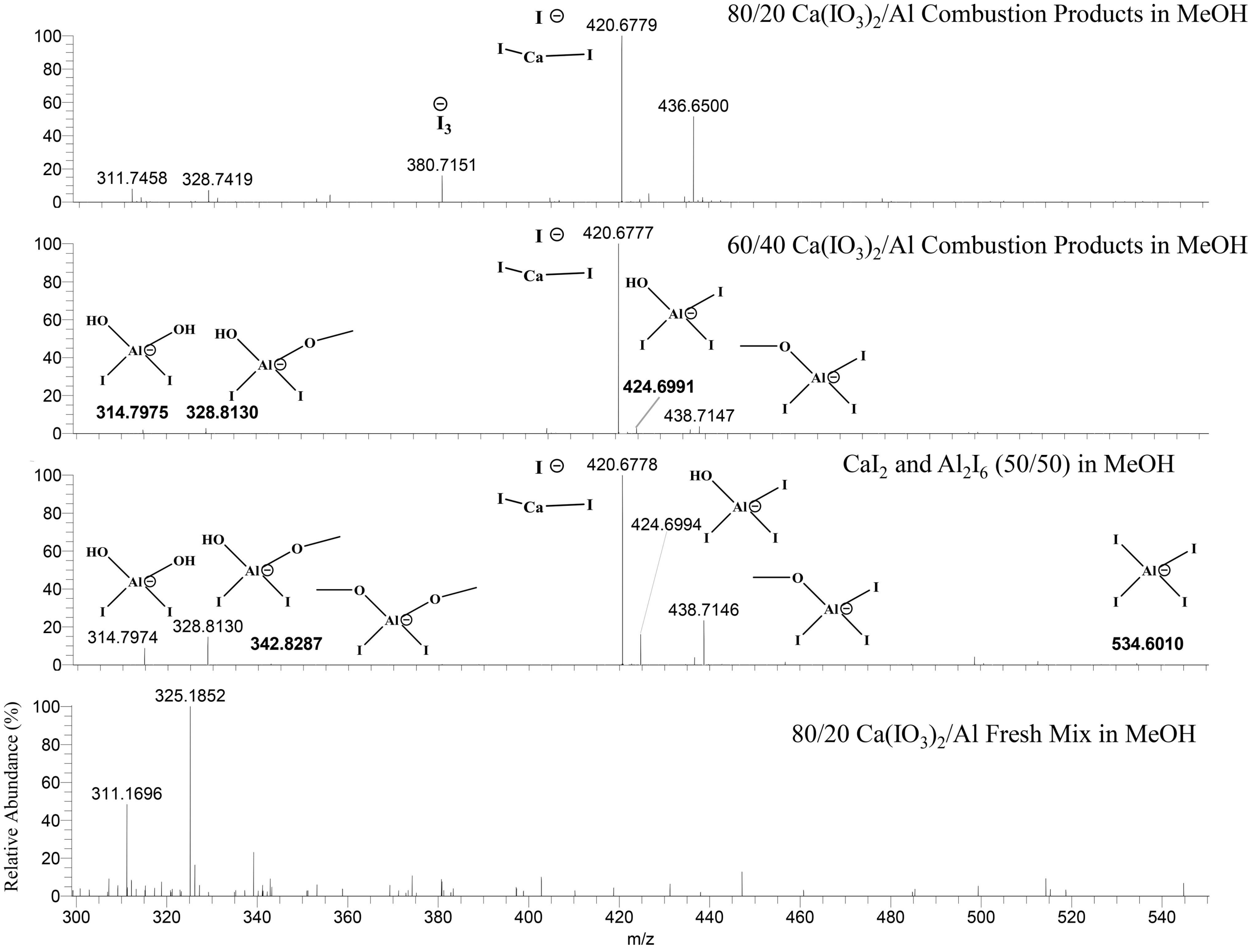

Figure 6. LC/MS of the Methanol Extract of 60/40 $Ca(IO_3)_2$ /Al Combustion products.

along with the great reduction in produced I_2 (42% with 20% Al down to 2% with 40% Al, see Tables 2 and 3) suggest some formation of Al_2I_6, a Lewis acid. The peak binding energies of the iodine signal from XPS suggests that the combustion products from $Ca(IO_3)_2$/Al (both 80/20 and 60/40) as well as other iodate/Al mixtures, contain iodine present as iodide (Table 4). [A similar trend was observed when combustion products from a 60/40 I_2O_5/Al mixture were analyzed on DSC/SDT, with a mass loss at 300 °C of 21%. No I_2 was observed from the extraction of the mixture with KI solution (and pH of the water solution was 4), which also suggests the formation of Al_2I_6.]

The occurrence of iodides in combustion products of Ca $(IO_3)_2$/Al and I_2O_5/Al, was confirmed by LC/MS of methanol and water extracts. Methanol extracts of 60/40 $Ca(IO_3)_2$/Al combustion products showed peaks consistent with CaI_2 (dominant) and Al_2I_6 (peaks of which were more prominent in methanol compared to water extracts, Figure S95), where methanol extracts of 80/20 $Ca(IO_3)_2$/Al combustion products showed peaks consistent with only CaI_2 (Figure 6). Similar peaks were observed in a standard methanol solution of 50/50 CaI_2/Al_2I_6. However, adding CaO to an aqueous or methanol standard solution of Al_2I_6 showed a decrease in Al_2I_6 signals, and the formation of CaI_2, suggesting that moisture might adversely affect the composition of the products if they contained a mixture of CaO and Al_2I_6 (Figure 7), promoting the formation of CaI_2. LC/MS of the water extract of 60/40 I_2O_5/Al combustion products shows peaks consistent with Al_2I_6 (Figure 8), but they were not observed in the 80/20 I_2O_5/Al combustion products. What is also interesting to note, is that the extract of a fresh mixture of 80/20 I_2O_5/Al produced LC/MS peaks consistent with known hydration products of I_2O_5 (IO_3^- from HIO_3, and $I_2O_5{\cdot}IO_3^-$ from $I_2O_5{\cdot}HIO_3$) [11]. The methanol extract of fresh 80/20 Ca $(IO_3)_2$/Al did not contain any identifiable peaks (Figures 6 and 8).

Impact, friction, and electrostatic discharge (ESD) sensitivity tests were conducted on the mixtures of $Ca(IO_3)_2$/Al because this mixture shows the most promise to be included in final formulations with polymers. Compared with RDX, this mixture is not sensitive to friction or impact, but does have a similar and sometimes more sensitive response

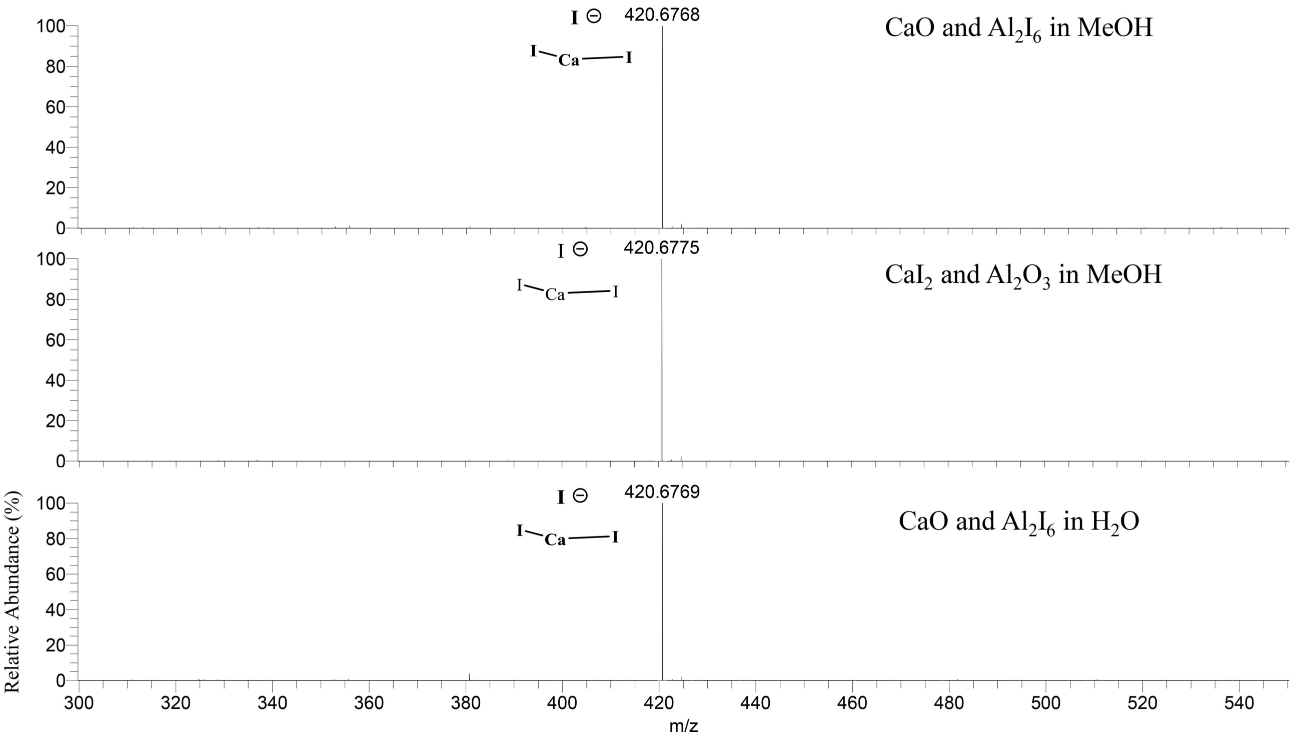

Figure 7. LC/MS of extracts of CaOand Al_2I_6.

Table 8. Sensitivity Testing.

Composition		%	% Al	BOE Impact H_{50} (cm)	BAM Friction TIL 1/6 (N)	ESD TIL 0/20 (J)
RDX		100	0	21,9	120	0,074
$Ca(IO_3)_2$ (−325mesh) Al (23μm Obron)	Ca $(IO_3)_2$	75	25	>75	360	0,085
$Ca(IO_3)_2$ (−325mesh) Al (23μm Obron)	Ca $(IO_3)_2$	90	10	>75	360	0,074
$Ca(IO_3)_2$ (−325mesh) Al (23μm Obron)	Ca $(IO_3)_2$	95	5	>75	>360	0,045
$Ca(IO_3)_2$ (−325mesh) Al (23μm Obron) + 20 % Polyurethane Foam (50-100mesh)	Ca $(IO_3)_2$	72	8	>75	>360	0,19

than RDX to ESD (Table 8). Adding a polyurethane binder did not change the impact or friction sensitivity, and seemed to improve the ESD sensitivity.

4 Conclusions

As a replacement for I_2O_5, calcium iodate [$Ca(IO_3)_2$] was unique among the iodine-containing salts examined (sodium, potassium, calcium and bismuth iodates and periodates of the alkali metals). When combusted with aluminum under argon, $Ca(IO_3)_2$ released the most molecular iodine and trapped the smallest amount of iodine as an iodide salt in an 80/20 mix with aluminum. In this mixture, calcium iodate reacted exothermically but did not release as much heat as some of the other iodate salts. More heat could be obtained by increasing the amount of aluminum, but this would have been at the cost of some molecular iodine. When 60/40 mixtures of I_2O_5/Al or $Ca(IO_3)_2$/Al were combusted, little or no molecular iodine was recovered. This and other evidence (SDT, XPS, XRD, LC/MS) suggested that with excess aluminum, aluminum triiodide (Al_2I_6) may have been formed from a reaction of the unburned aluminum and free iodine in this inert atmosphere. It has been reported that the completeness of reaction of a stoichiometric mixture of I_2O_5/Al is pressure dependent (at pressures less than atmospheric). The reaction forms more Al_2O_3 rather than Al_2I_6 as atmospheric pressure is approached [18]. We have studied 80/20 $Ca(IO_3)_2$/Al, $Bi(IO_3)_3$ /Al, and NaIO3/Al at both 515 kPa (60 psig) and 2515 kPa (350 psig)

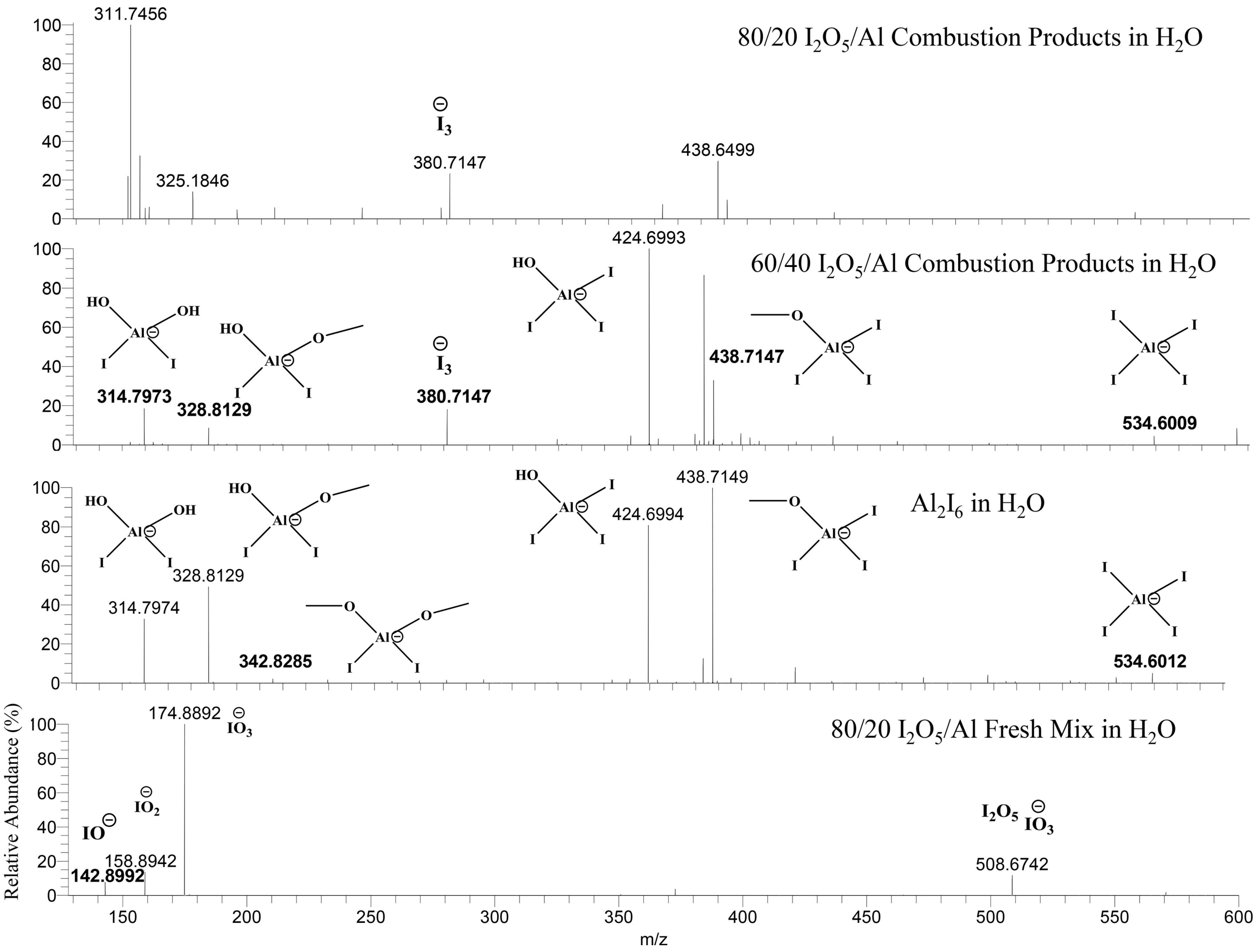

Figure 8. LC/MS of the H2O Extract of 60/40 I2O5/Al Combustion products.

pressures (Table 2) to determine if the reaction can be driven to produce more molecular iodine. Interestingly, 80/20 Bi$(IO_3)_3$/Al produced very little free iodine (possibly further combination of Bi$+I_2$); 80/20 $Ca(IO_3)_2$/Al produced slightly more iodine (45% vs. 42%); and 80/20 $NaIO_3$/Al produced considerably more iodine (28% vs. 16%). The increase in iodine produced from 80/20 $NaIO_3$/Al would likely be coming from further oxidation of NaI.

Table 9 summarizes the reactions observed with the various iodate and periodate salts. The production of molecular iodine is opposed by both the potential for the original cation (Na^+, K^+, Ca^{2+}, Bi^{3+}) as well as the aluminum to form the iodide salts. Aluminum preferentially forms the oxide if there is sufficient oxygen available in the mixture, but the alkali ions preferentially form the iodide (MI), reducing molecular iodine formation. Calcium and bismuth form oxides, but bismuth oxide undergoes a metathesis reaction with aluminum to form, ultimately, bismuth iodide, which probably forms through elemental bismuth reacting with elemental iodine. In aluminum heavy mixtures, calcium iodate may form calcium iodide and aluminum iodide, although it is difficult to tell the difference between having calcium oxide and aluminum iodide in the products (with post reaction with moisture to form $CaI_2·6.5H_2O$), or having a mixture of calcium and aluminum iodides. In general, excess aluminum reduces I_2 formation.

Table 9. Reactions of Iodine Salts with 20% Al in Argon (dominant products are highlighted).

MIO_3	+	Al	→	Al_2O_3		Al_2I_6		MI		MO		I_2
I_2O_5	+	Al	→	Al_2O_3								I_2
$NaIO_4$												
↓												
$NaIO_3$	+	Al	→	Al_2O_3			+	NaI	+	Na_2O	+	I_2
KIO_4												
↓												
KIO_3	+	Al	→	Al_2O_3			+	KI	+	K_2O	+	I_2
$Ca(IO_3)_2$	+	Al	→	Al_2O_3					+	CaO	+	I_2
$Bi(IO_3)_3$	+	Al	→	Al_2O_3	+	Bi	+	BiI_3	+	Bi_2O_3	+	I_2

The fact that more molecular iodine is released when there is more oxygen available to the fuels indicates that

Table 10. Thermodynamic Calculations of Oxygen Exchange.

Potential for Metal Iodide Oxidation to I_2					Potential for Metal Oxide O_2 exchange with Aluminum				
	ΔG (kJ/mol)	ΔS (J/mol/K)	ΔH (kJ/mol)			ΔG (kJ/mol)	ΔS (J/mol/K)	ΔH (kJ/mol)	
2	MI	+	0,5	$O_2 \rightarrow 1\ I_2(g) + 1\ M_2O$	3	M_2O	+	2	$Al \rightarrow 1\ Al_2O_3 + 6\ M$
NaI	216	36	224		Na_2O	−456	77	−433	
KI	347	40	357		K_2O	−616	100	−591	
1	MI_2	+	1	$O_2 \rightarrow 1\ I_2(g) + 1\ MO$	3	MO	+	2	$Al \rightarrow 1\ Al_2O_3 + 3\ M$
CaI_2	−55	54	−39		CaO	228	5	229	
MgI_2	−192	55	−175		MgO	126	11	129	
2	MI_3	+	2	$O_2 \rightarrow 3\ I_2(g) + 1\ M_2O_3$	1	M_2O_3	+	2	$Al \rightarrow 3\ Al_2O_3 + 1\ M$
BiI_3	−85		−512		Bi_2O_3	−4253	1	−4453	
AlI_3	−923	207	−861						

most of the metals would rather be oxides than iodides. This is supported by the Gibbs free energy and enthalpy of oxidation of iodide salts to metal oxides (Table 10). The oxidation of the alkali iodide salts is endothermic, with a positive Gibbs free energy suggesting that they are less likely to produce iodine gas than the other iodide salts listed. The oxidation of the alkali earth iodides, aluminum iodide, and bismuth iodide is exothermic, with a negative Gibbs free energy suggesting release of iodine to be more favorable than that of the alkalis. All the iodide salts (KI, NaI, CaI_2, BiI_3, and Al_2I_6) were run on SDT under air as well as under nitrogen. Under air, calcium iodide and aluminum iodide produced traces with small exotherms and large mass losses. In contrast, under nitrogen, calcium iodide showed no decomposition as heat flow and mass loss below its melting point, and aluminum iodide produced an endotherm during its melt with some significant mass loss (moderate sublimation). These differences suggest significant oxidation in air for these two salts. The sodium, potassium, and bismuth iodide salts showed little difference between air and nitrogen, with their melts accompanying almost total mass loss, which is presumed to be mostly sublimation (Table 7).

The potential for molecular iodine to be released may depend on the relative oxyphilicity of aluminum relative to the cation accompanying the iodate (Table 10). This would especially be important in oxygen deficient situations such as experiments performed under inert atmosphere. With insufficient oxygen the iodide may be formed instead. We believe this to be the case with bismuth iodate, due to the favorable reaction between bismuth oxide and aluminum, which frees up bismuth for a reaction with iodine. Because the reaction of some metal oxides (calcium and magnesium) with aluminum is not as favorable, it is likely that excess aluminum in this case would react with iodine directly in an oxygen deficient environment.

We have noted that use of a combination of boron carbide (B_4C) and aluminum as fuels resulted in more iodine formation from the alkali iodates than the use of either fuel alone (Table 2). The exact nature of the reactions have not been ascertained. Boron carbide has been examined by bomb calorimetry, and diboron trioxide and carbon dioxide were formed [19,20].

$$B_4C + 4O_2 \rightarrow 2B_2O_3 + CO_2 \tag{7}$$

Furthermore, the combustion products of boron with potassium nitrate and potassium perchlorate under argon were found to be $KB_5O_8{\cdot}4H_2O$ and $KB_5O_6(OH)_4{\cdot}2H_2O$, respectively [21]. The authors of that article speculate that reaction 8 occurs:

$$2KClO_4 + 2B \rightarrow 2KBO_2 + Cl_2 + 2O_2 \tag{8}$$

Using that model we suggest a similar reaction (eq 9). Indeed, over time a boron carbide mixture with sodium iodate evolved molecular iodine at room temperature. Perhaps the reason the combination fuel Al/B_4C results in higher amounts of evolved I_2 can be attributed to the alkali metal being removed from the competition with aluminum for the freed oxygen. Thus, both the alkali metal and the aluminum are incorporated in a stable species allowing molecular iodine to be evolved.

$$4\ KIO_3 + B_4C \rightarrow 4\ KBO_2 + CO_2 + 2\ I_2 + O_2 \tag{9}$$

Acknowledgements

The authors gratefully acknowledge DTRA for funding this work through grant HDTRA1-14-0027.

References

[1] J. C. Oxley, J. L. Smith, M. Donnelly, M. Porter, "Fuel-oxidizer mixtures: their stabilities and burn characteristics" *J. Therm. Anal. Calorim.* **2015**, *121*, 743–763.

[2] R. Tennen, B. Setlow, K. L. Davis, C. A. Loshon, P. Setlow, "Mechanisms of killing spores of Bacillus subtilis by iodine, glutaraldehyde, and nitrous acid" *J. Appl. Microbiol.*, **2000**, *89*, 330–338.

[3] B. R. Clark, M. L. Pantoya, "The aluminum and iodine pentoxide reaction for the destruction of spore forming bacteria" *Phys. Chem. Chem. Phys.*, **2010**, *12*, 12653–12657.

[4] H. Wang, G. Jian, W. Zhou, J. B. DeLisio, V. T. Lee, M. R. Zachariah, "Metal Iodate-Based Energetic Composites and Their Combustion and Biocidal Performance" *ACS Appl. Mater. Interfaces.* **2015**, *7*, 17363–17370.

[5] A. E. Burgess, J. C. Davidson, Kinetics of the Rapid Reaction between Iodine and Ascorbic Acid in Aqueous Solution using UV-Visible Absorbance and Titration by and Iodine Clock" *J. Chem. Educ.* **2014**, *91*, 300–304.

[6] A. J. Adrian, D. N. Hume, "A Spectrophotometric Investigation of Bismuth Iodide Complexes" *Inorg. Chem.* **1967**, *6*, 331–339.

[7] T. Urabe, M. Tanaka, S. Kumakura, T. Tsugoshi, "Study on chemical speciation in aluminum chloride solution by ESI–Q-MS" *J. Mass. Spec.* **2007**, *42*, 591–597.

[8] United Nations, "Recommendations on the Transport of Dangerous Goods, Manual of Tests and Criteria," Fifth revised edition, **2009**.

[9] MIL-STD-1751A, ARDEC Method 1032.

[10] J. C. Poret, A. P. Shaw, C. M. Csernica, K. D. Oyler, J. A. Vanatta, G. Chen, "Versatile Boron Carbide-Based Energetic Time Delay Compositions" *ACS Sustainable Chem. Eng.*, **2013**, *1*, 1333–1338.

[11] B. K. Little, S. B. Emery, J. C. Nittinger, R. C. Fantasia, C. M. Lindsay, Physiochemical Characterization of Iodine(V) Oxide, Part 1: Hydration Rates" *Propellants Explos. Pyrotech.* **2015**, *40*, 595–603.

[12] K. H. Stern, "High Temperature Properties and Decomposition of Inorganic Salts Part 4. Oxy-Salts of Halogens" *J. Phys. Chem. Ref. Data.* **1974**, *3*, 481–526.

[13] G. W. Watt, J. L. Hall, "Aluminum Iodide" *Inorg. Synth.* **1953**, *4*, 117.

[14] J. Erdey, J. Simon, S. Gal, "Thermoanalytical properties of analytical grade reagents-V. Sodium Halates" *Talanta.* **1968**, *15*, 653–661.

[15] B. Bentria, D. Benbertal, M. Bagieu-Beucher, R. Masse, A. Mosset, "Crystal structure of anhydrous bismuth iodate, $Bi(IO_3)_3$" *J. Chem. Crystallogr.* **2003**, *33*, 867–873.

[16] D. Lide, (editor) "CRC Handbook of Chemistry Physics" 85th ed, CRC Press, **2004**.

[17] J. Bousquet, P. Vermande, "Ètude du mécanisme de la décomposition thermique de l'iodate de calcium anhydre" *Soc. Chim. Mémoires.* **1964**, *5*, 214–218.

[18] V. G. Ivanov, G. V. Ivanov, P. V. Lapin, V. P. Kuznetso, "Role of Iodation in the Combustion of Metal Oxides with Iodine Pentoxide" *Fizika Goreniya 1 Vzryva.* **1980**, *27*, 28–36.

[19] L. M. Litz, R. A. Mercuri, "Oxidation of Boron Carbide by Air, Water, and Air-Water Mixtures at Elevated Temperatures" *J. Electrochemical Soc.* **1963**, *110*(8), 921–925.

[20] E. S. Domalski, G. T. Armstrong, "The Heat of Formation of Boron Carbide" *Journal of Research of the National Bureau of Standards – A. Physics and Chemistry.* **1968**, *72*A(2), 133–139.

[21] P.-J. Liu, L.-L. Liu, G.-Q. He, "Effect of solid oxidizers on the thermal oxidation and combustion performance of amorphous boron." *J. Therm. Anal. Calorim.* **2016**, *124*, 1587–1593.

Received: February 1, 2017
Revised: May 23, 2017

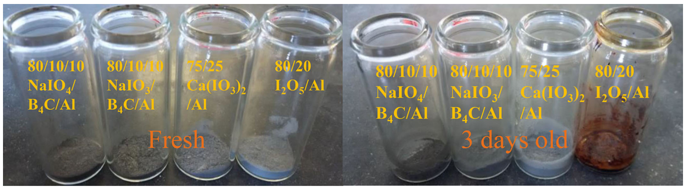

J. C. Oxley, J. L. Smith, M. M. Porter, M. J. Yekel, J. A. Canaria*

1 – 18

Potential Biocides: Iodine-Producing Pyrotechnics